

A Model of Nuclear Recoil Scintillation Efficiency in Noble Liquids

D.-M. Mei ^{a,*} Z.-B. Yin ^{a,b,1}, L.C. Stonehill ^c, A. Hime ^c

^a*Department of Physics, The University of South Dakota, Vermillion, South Dakota 57069*

^b*Institute of Particle Physics, Huazhong Normal University, Wuhan 430079, China*

^c*Los Alamos National Laboratory, Los Alamos, NM 87545*

Abstract

Scintillation efficiency of low-energy nuclear recoils in noble liquids plays a crucial role in interpreting results from some direct searches for Weakly Interacting Massive Particle (WIMP) dark matter. However, the cause of a reduced scintillation efficiency relative to electronic recoils in noble liquids remains unclear at the moment. We attribute such a reduction of scintillation efficiency to two major mechanisms: 1) energy loss and 2) scintillation quenching. The former is commonly described by Lindhard's theory and the latter by Birk's saturation law. We propose to combine these two to explain the observed reduction of scintillation yield for nuclear recoils in noble liquids. Birk's constants kB for argon, neon and xenon determined from experimental data are used to predict noble liquid scintillator's response to low-energy nuclear recoils and low-energy electrons. We find that energy loss due to nuclear stopping power that contributes little to ionization and excitation is the dominant reduction mechanism in scintillation efficiency for nuclear recoils, but that significant additional quenching results from the nonlinear response of scintillation to the ionization density.

Key words: Nuclear Recoil, Dark matter detection, Relative Scintillation Efficiency

PACS: 95.35.+d, 11.10.Lm, 29.40.Mc

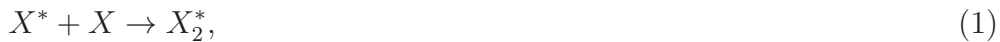
* Corresponding author.

Email address: Dongming.Mei@usd.edu (D.-M. Mei).

¹ Permanent Address: Institute of Particle Physics, Huazhong Normal University, Wuhan 430079, China

1 Introduction

Noble liquid scintillators such as liquid xenon [1], argon [2,3], and neon [4] are expected to be excellent targets and detectors for direct dark matter detection experiments searching for Weakly Interacting Massive Particles (WIMPs), which may constitute the dark matter in the universe [5,6,7,8]. These experiments measure scintillation light induced by low-energy nuclear recoils due to elastic scattering of WIMPs. Absorption of nuclear recoil energy in noble liquid scintillators produces excitons and electron-ion pairs along the track. Free excitons collide with ground states to form excited molecules (excimers) through



where X stands for any type of noble liquid. Free ions undergo collision, recombination and deexcitation processes,



to form excimers. The excimers then decay radiatively from the lowest-excited molecular states $^1\Sigma_u^+$ and $^3\Sigma_u^+$ to the repulsive ground state $^1\Sigma_g^+$.

It is well known that noble liquid scintillators have reduced scintillation yield for low-energy nuclear recoils compared to electronic recoils [9,10,11,12,13,14]. Only a fraction of the energy loss results in ionization and atomic excitation. Moreover, high ionization density undermines recombination of electron-ion pairs and reduces scintillation light yield. The relative scintillation yield, defined as the ratio of the numbers of photons emitted from pure noble liquids in nuclear and electronic recoil events at the same energy, is a good measurement of the nuclear recoil scintillation efficiency, q_f , determined by the visible deposited energy over the true recoil energy. In the case of electrons and γ -rays, almost all the energy loss by ionization is converted into scintillation light through electron-ion recombination, so the relative scintillation efficiency is assumed approximately equal to 1 in the absence of an electric field. But in the case of nuclear recoils, q_f is much smaller than 1 and can vary as a function of nuclear recoil energy.

The scintillation efficiency plays an important role in the direct detection of WIMPs. In the design of a new experiment, the scintillation efficiency is related

to the detection threshold and hence to the background level and ultimate sensitivity. In the interpretation of an experimental result, the scintillation efficiency is crucial to the determination of WIMP mass and WIMP-nucleon cross section. The nuclear recoil scintillation efficiencies for liquid xenon, argon, and neon have been measured [9,10,11,12,13,14] using neutron sources. The detector is usually calibrated with well-known γ -rays, such as 122 keV and 133 keV lines from a ^{57}Co source. The relative scintillation efficiency for γ -rays, ϵ_γ , is defined as the visible energy divided by the incident γ -ray energy, and is assumed to be 1. As discussed later in this paper, this assumption is valid for electronic recoil energy above 20 keV in the noble liquids under investigation. The nuclear recoil scintillation efficiency is determined by the ratio of the nuclear recoil visible energy using the electron-equivalent energy calibration to the true recoil energy E_R , $q_f = E_R^{\text{vis}}/E_R$.

The measurements are usually compared to either Lindhard's theory [15] or Hitachi's treatment [16]. It was found that Lindhard's theory alone can not well explain the observed behavior in the data. The alternative explanation, Hitachi's treatment, states that a biexcitonic quenching mechanism can occur before the free excitons self-trap when the excitation density is very high. This explanation can agree reasonably well with the xenon data [9], but has not been applied to explain low-energy recoil data for neon or argon. Moreover, there are other possible quenching processes that could contribute to the reduction of scintillation efficiency for low-energy nuclear recoils. These include collisions (via the Penning process [17]) between two excited molecular states (excimers) to form one excited state and one ground state [18], and supereleastic collisions that quench the singlet states to triplet states [19].

A more universal description of the reduced scintillation efficiency for nuclear recoils is preferred for all noble liquid scintillators. Since the proposed quenching mechanisms are all dependent on the density of the ionization and excitation track left by the recoiling nucleus, it is possible to form a combined model of these mechanisms without incorporating details of the relative contributions of the different mechanisms. Birk's saturation law for organic scintillators [20] provides a convenient description of the dependence of scintillation quenching on ionization density. In this study, we apply Birk's law to noble liquids, offering a conventional way to determine the total scintillation efficiency of nuclear recoils by measuring Birk's constant (kB). It has been shown that the luminescence intensity in the noble gas scintillator depends solely on the energy density and is independent of the kind of the particle [21,22]. This is to say that a measurement of kB for noble liquids will allow understanding of the relative scintillation efficiency for nuclear recoils induced by neutrons, alphas, and other heavy isotopes. This is a very valuable way to determine the scintillation efficiency for nuclear recoils induced by all types of particles in noble liquid scintillators. Furthermore, this method allows determination of the relative scintillation efficiency for nuclear recoils in noble liquids by

measuring the constant kB with γ -rays. This is a much easier measurement compared to the nuclear recoil measurements with neutron and alpha sources.

In this paper, we propose a model to combine Lindhard's theory and Birk's saturation law to describe the reduction in scintillation efficiency observed in noble liquid scintillators. We describe these two reduction mechanisms in Section 2 and 3, respectively. The model combining these two reduction mechanisms is presented in Section 4 and its predictions are compared to experimental data in Section 5. The scintillation efficiency (ϵ_γ as a function of recoil energy) for very low-energy electrons and γ -rays is discussed briefly in Section 6. Finally, we summarize our conclusions in Section 7.

2 Reduced Ionization Energy by Nuclear Collisions

When a neutron or WIMP scatters elastically off a noble liquid atomic nucleus, the recoiling nucleus then loses its energy by colliding with electrons and nuclei within the detector. This nuclear recoil process involves the competition between, on the one hand, energy transfer to atomic electrons and, on the other hand, energy transfer to translational motion of atoms. The total rate at which the recoiling nucleus loses energy with respect to distance (dE/dx) is dependent on the medium through which it travels, and is also called the stopping power. At low energies, the total stopping power of the noble liquid atom consists of electronic and nuclear stopping power. The electronic stopping power is the amount of energy per unit distance that the recoiling nucleus loses due to electronic excitation and ionization of the surrounding noble liquid atoms. The nuclear stopping power is the energy loss per unit length due to atomic collisions that contribute to the kinetic energy (thermal motion) of the noble liquid atoms, but that do not result in internal excitation of atoms. The proportion of electronic to nuclear stopping power depends on the recoil energy of the nucleus. If the recoil energy were very large, the nuclear stopping power would be very small compared to the electronic stopping power. However, in the energy range of WIMP-nucleus elastic scatterings, the nuclear stopping power plays a significant role in the energy loss of the recoiling noble liquid nucleus. J. Lindhard *et al.* [15] discussed in detail the theory of energy loss of low-energy nuclei.

Supposing that the recoiling nucleus loses all of its energy in the detector, the total energy loss can be expressed in terms of the losses due to the electronic stopping power η and nuclear stopping power ν as [15]

$$E_R = \eta(E_R) + \nu(E_R), \tag{3}$$

where η and ν are both functions of recoil energy E_R . As only the portion of

the energy lost in electronic excitation or ionization will result in the creation of excitons and electron-ion pairs in the noble liquids, the fraction defines an ionization energy reduction factor (f_n) due to losses to the nuclear stopping power

$$f_n(E_R) \equiv \frac{\eta(E_R)}{E_R} = \frac{\eta(E_R)}{\eta(E_R) + \nu(E_R)}. \quad (4)$$

As the total stopping power is

$$\left(\frac{dE}{dx}\right)_{\text{tot}} = \left(\frac{dE}{dx}\right)_{\text{elec}} + \left(\frac{dE}{dx}\right)_{\text{nucl}}, \quad (5)$$

$f_n(E_R)$ can then be determined by the ratio of two integrals

$$f_n(E_R) = \frac{\int_0^{E_R} (dE/dx)_{\text{elec}} dE}{\int_0^{E_R} ((dE/dx)_{\text{elec}} + (dE/dx)_{\text{nucl}}) dE}. \quad (6)$$

To present f_n as a function of recoil energy, the integrals above should be evaluated for each possible recoil energy. Lindhard *et al.* [15] represents f_n as

$$f_n = \frac{kg(\varepsilon)}{1 + kg(\varepsilon)}, \quad (7)$$

where, for a nucleus of atomic number Z , $\varepsilon = 11.5E_R$ (keV) $Z^{-7/3}$, $k = 0.133Z^{2/3}A^{-1/2}$, and $g(\varepsilon)$ is well fitted by: $g(\varepsilon) = 3\varepsilon^{0.15} + 0.7\varepsilon^{0.6} + \varepsilon$. Fig. 1 shows this ionization energy reduction factor for noble liquids from Lindhard's theory.

3 Reduced Scintillation Yield due to High Ionization Density

3.1 Birk's Saturation Law

The passage of a particle in a noble liquid produces a structured track along its path that is conveniently described in terms of a core and a penumbra [23]. The penumbra that surrounds the core is a low ionization density zone. The core is expected to be a high ionization density zone, so ionization density dependent quenching caused by biexcitonic collisions or the Penning process is likely to occur there. On the one hand, the free excitons can be self-trapped to form excimers, for example, Ar_2^* , that then fluoresce to the lowest states. On the

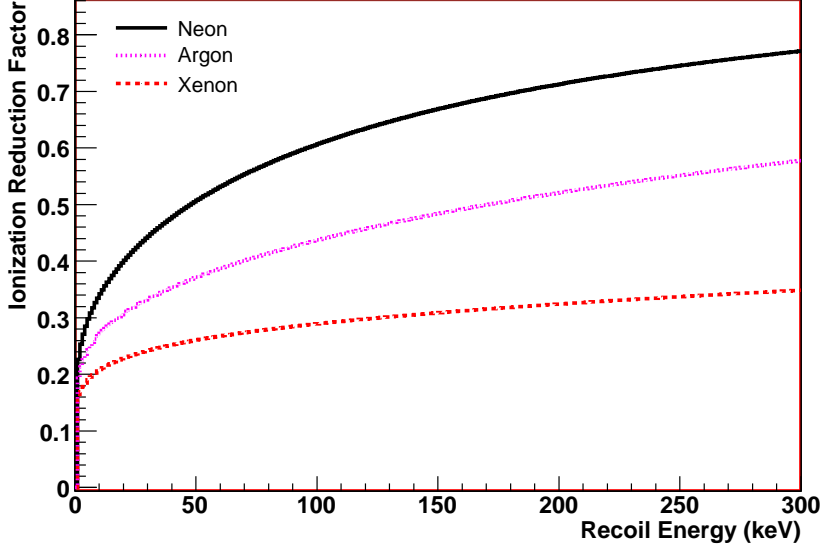


Fig. 1. The ionization energy reduction factor according to Lindhard's theory versus the recoil energy in liquid neon (black line), argon (red dotted line) and xenon (magenta dashed line).

other hand, the free excitons can diffuse and undergo biexcitonic quenching, or the excimers can further collide with each other via the Penning process, with a probability of occurrence that depends on the density of free excitons produced, which is proportional to ionization density. Therefore, the biexcitonic collisions and the Penning process act as quenching agents for the excitons produced by the ionization along the track. It is well known that the number of excitons and electron-ion pairs produced per unit path length is proportional to the electronic energy loss dE/dx [24], with a proportionality constant that will be designated as A . The local concentration of the core is also proportional to the ionization density, and is given by BdE/dx . The overall collision probability in the core is given by k . Thus, the specific fluorescence can be expressed by

$$\frac{dS}{dx} = \frac{A \frac{dE}{dx}}{1 + kB \frac{dE}{dx}}. \quad (8)$$

Eq. 8 is called Birk's saturation law [20], which describes the relative scintillation response of scintillators to an ionizing particle of any energy. The values of A and kB can be determined experimentally.

According to Eq. 8, the scintillation photon yield is reduced at high ionization density. Thus, we define a quenching factor

$$f_l = \frac{1}{1 + kB \frac{dE}{dx}}, \quad (9)$$

which is related to the electronic stopping power dE/dx induced by nuclear recoils.

3.2 Electronic Stopping Power for Heavy Ions

For ions heavier than protons, the electronic stopping power in a given material can be calculated from the stopping power in the same material based on the ‘‘heavy ion scaling rule’’,

$$S_A = (\zeta Z_1)^2 S_p, \quad (10)$$

where the stopping power S_p for protons is determined at the same velocity as the stopping power S_A for heavy ions. ζZ_1 is the ‘effective charge’ for ions of atomic number Z_1 . Effective ion charges will result from the stripping of bound electrons from the ion when moving through a medium. Thus, the effective charge fraction ζ is expected to be related to the relative velocity, v_r , between the ion velocity v_1 and the velocity of the valence electrons in the medium. When the valence electron gas of the medium is characterized by the effective number of electrons that participate in plasma excitations, the velocity of the valence electrons can be characterized by the Fermi velocity $v_F = (3\pi^2 n)^{1/3} \hbar/m$, where n is the electron density and m the electron mass. v_r is proposed in [25] to be

$$v_r = \begin{cases} \frac{3}{4} v_F (1 + \frac{2}{3} \frac{v_1^2}{v_F^2} - \frac{1}{15} \frac{v_1^4}{v_F^4}), & \text{if } v_1 \leq v_F \\ v_1 (1 + \frac{1}{5} \frac{v_F^2}{v_1^2}), & \text{if } v_1 > v_F. \end{cases} \quad (11)$$

A formula for the effective charge fraction ζ has been deduced by Brand and Kitagawa [26] as a good approximation in the region where stopping power is proportional to the velocity v_1 :

$$\zeta = q + 0.5(1 - q) \ln [1 + (\frac{2\Lambda v_F}{1.919 v_0 a_0})^2], \quad (12)$$

where v_0 and a_0 are the Bohr velocity and radius, respectively. q denotes the degree of ionization, which was calculated by applying a velocity-stripping criterion to the Thomas-Fermi model [27] of the neutral atom and is tabulated as a function of the reduced variable $y_r = v_r/(Z_1^{2/3} v_0)$ in [26]. An alternative energy stripping criterion was proposed by Mathar and Posselt (MP) [28] to explain the dependence of the ionization fraction on the ion velocity and to yield better results especially for higher ion velocities. Using the energy

definition of the Brandt-Kitagawa (BK) model, q is determined by solving numerically the following equation

$$6a(1-q)^{2/3}y^2 = \frac{q(6+q)}{7}, \quad (13)$$

where $a \equiv 0.24005$ and $y \equiv v_1/(v_0Z^{2/3})$. The screening radius Λ , which is used to parameterize the charge density profile of the projectile ion, is determined by minimizing the total energy of the bound electrons in BK to be

$$\Lambda = \frac{2a(1-q)^{2/3}a_0}{Z_1^{1/3}[1-(1-q)/7]}. \quad (14)$$

Ziegler, Biersack and Littmark (ZBL) [29] modified the ion size parameter Λ to include a tabulated factor individual to Z_1 . The ionization fraction q is then parameterized as a universal fitting function of y_r as

$$q = 1 - e^{(0.803y_r^{0.3} - 1.3167y_r^{0.6} - 0.38157y_r - 0.008983y_r^2)}. \quad (15)$$

The ionization fractions from the three different approaches described above are reproduced in Fig. 2 as a function of the variables y or y_r . In this paper, we adopt the BK formalism to calculate the effective charge of ions and the electronic stopping power values, but the alternative approaches are used to estimate the theoretical uncertainties.

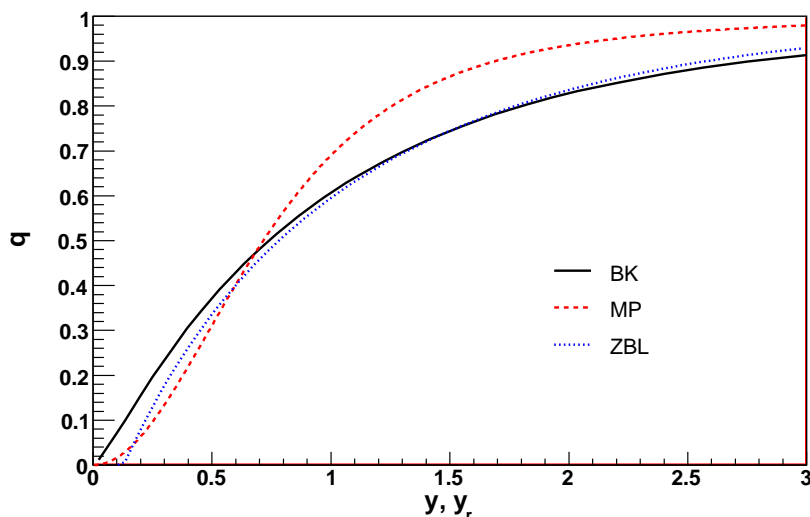


Fig. 2. Ionization fraction as a function of variable y or y_r in the BK (black solid line), ZBL (blue dotted line) and MP (red dashed line) models.

We can utilize Eq.10 and the effective ion charge to calculate the electronic stopping power, provided that the stopping power values for protons in the

same material are known. A table of stopping powers and ranges for protons and alpha particles has been produced by a committee of the International Commission on Radiological Units and Measurements (ICRU) [30]. In the present study, we retrieve the proton stopping powers from the PSTAR database [31]. Fig. 3 shows the electronic stopping power for proton projectiles in Ar target as a function of the proton velocity $\beta \equiv v/c$. According to Lindhard and Scharff [32], the stopping power at low energy is proportional to the projectile velocity. This is illustrated by a proportional function (red thick line) fit in Fig. 3. We will use this fitting function to estimate the stopping power at lower energy, where it is not covered by the databases, to produce the electronic stopping power for ions at kinetic energy as low as 1 keV.

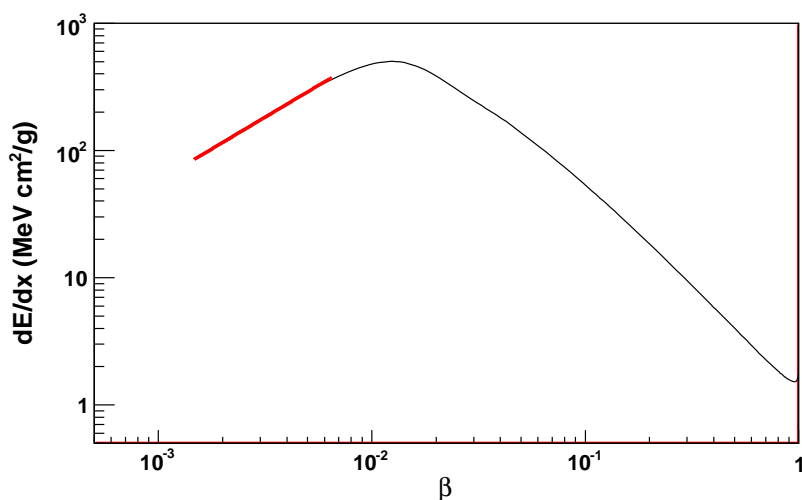


Fig. 3. Electronic stopping power for protons in an Ar target versus the velocity $\beta \equiv v/c$ of the proton projectiles. A proportional function (red thick line) is fitted to the low velocity region with a parameter of $5.776 \times 10^4 \pm 349.7$ MeV cm²/g.

Fig. 4 gives the electronic stopping power for Ar ions in Ar targets. The red solid line is produced based on BK model and the “heavy ion scaling rule”. Paul and Schinner (PS) [33] performed a systematic comparison of a large collection of stopping power data for projectiles from ³Li to ¹⁸Ar to those for alpha particles in the same materials. They found that, for each target element, a slightly adapted sigmoid function with three parameters can describe the normalized relative stopping power

$$S_{\text{rel}} = \frac{S_A/Z_1^2}{S_{\text{He}}/2^2}. \quad (16)$$

For comparison, results from the PS empirical scaling approach have also been plotted in Fig. 4 with a blue dashed line. The difference between the two calculations is about 10% at kinetic energy of 1 MeV and increases to 35% at

10 keV. In addition, a green dash-dotted line in the figure shows a calculation based on the “SRIM” program of Ziegler [29]. The results deviate from those of the BK and PS approaches at higher energy with a kink at ~ 0.1 MeV, but are comparable to the results of the BK model at lower energy.

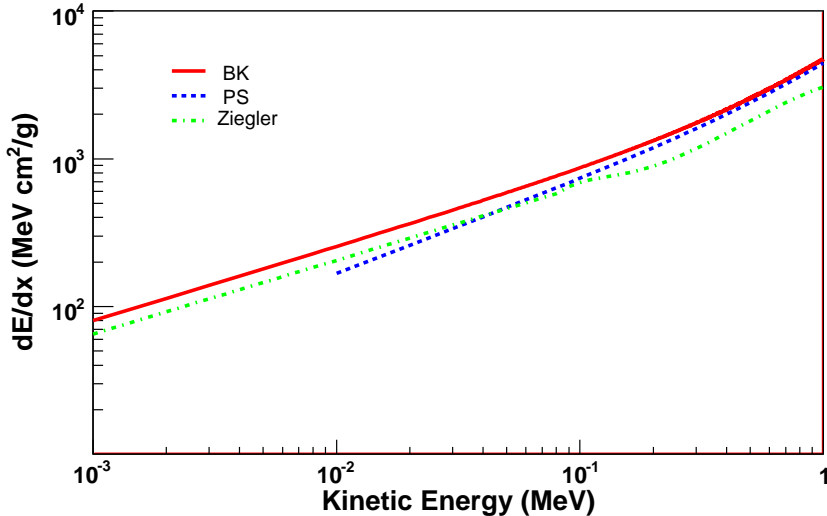


Fig. 4. Electronic stopping powers for Ar ions in Ar targets as a function of the kinetic energy. The red solid line is from the BK model, the blue dashed line from the PS empirical scaling approach and the green dash-dotted line from Ziegler’s SRIM program.

Based on the BK model, we show in Fig. 5 the electronic stopping power for Ar (black solid line), Ne (blue dotted line) and Xe (red dashed line) ions with themselves as the target materials. By comparing different effective ion charge calculation scenarios, the theoretical uncertainties on the stopping power values are estimated to be about 15% at 1 MeV and increase to about 50% at 1 keV where the theoretical description is known to become less reliable.

4 Model Prediction

The fraction of nuclear recoil energy, f_n (see Eq. 7), described in Section 2 ionizes or excites atoms in noble liquids. Ionizing particles produce excitons, electron-ion pairs, and a localized concentration core along the track. There are two cases: 1) free excitons form excimers through a self-trapping process [34,35,36], and 2) the ions are localized through the formation of excited molecular ions and eventually form excimers through recombination, deexcitation, and collision. The origins of the luminescence for both cases are attributed [37,38] to low excited molecular states, namely, $^1\Sigma_u^+$ or $^3\Sigma_u^+$. The fraction of excitons that undergo self-trapping depends largely on ionization

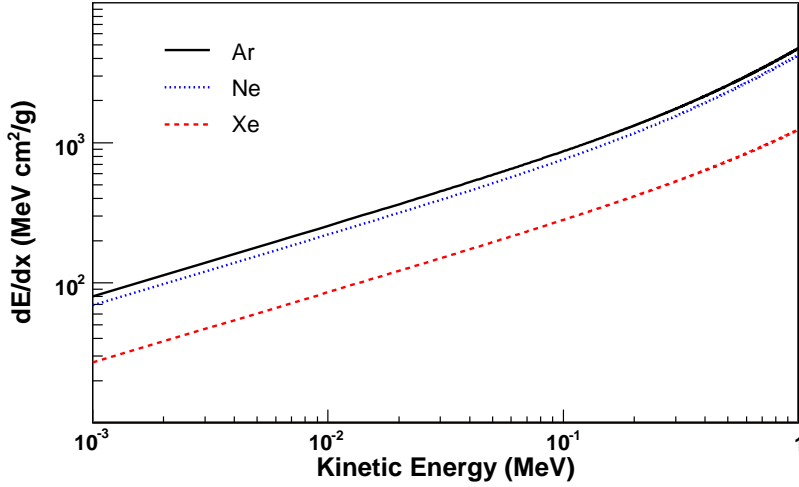


Fig. 5. The electronic stopping powers based on the BK model for Ar (black solid line), Ne (blue dotted line) and Xe (red dashed line) ions with themselves as the target materials.

density. The fraction of ions that combine with ground states to form excited molecular ions is proportional to ionization density. Furthermore, the fraction of excimers relaxing to the lowest-excited states is also a function of ionization density. This is to say that some of the excitons or ions can collide each other without going to excimers and some of the formed excimers can further undergo the Penning process to reduce the number of radiative lowest-excited states. This part of excitons, ions, and the formed excimers is quenched. The quenching factor, f_l , is expressed in Eq. 9. Since f_n and f_l are independent of each other, the total scintillation efficiency in noble liquids can be represented by

$$q_f = f_n \times f_l. \quad (17)$$

We calculated f_n , the fraction of nuclear recoil energy that contributes to the ionization process in noble liquids, as a function of nuclear recoil energy, as shown in Fig. 1. The fraction of the collided excitons or ions, kB , is determined from experimental data based on Birk's saturation law by using Eq. 9.

- For liquid argon, $kB = 7.4 \times 10^{-4} \text{ MeV}^{-1} \text{ g cm}^{-2}$. This is determined by using a quenching factor (46%) from a heavy ion measurement [39], and dE/dx (1586.4 MeV cm²/g corresponds to 31.9 MeV/amu) is calculated by this work.
- For liquid neon, the Birk's constant, $kB = 1.12 \times 10^{-3} \text{ MeV}^{-1} \text{ g cm}^{-2}$, is determined by using a quenching factor measured in Ref. [14] with the dE/dx values calculated by this work.

- For liquid xenon, the quenching factor has been measured by several groups [9,10,11]. We use the measured quenching factor corresponding to a 70-keV recoil energy in Ref. [10] to determine the Birk's constant kB to be $2.015 \times 10^{-3} \text{ MeV}^{-1} \text{ g cm}^{-2}$.

The quenching factor due to scintillation quenching, f_i , is then calculated according to Eq. 9 for argon, neon and xenon. Multiplying these two reduction factors results in the total scintillation efficiency (Eq. 17) as shown in Fig. 6.

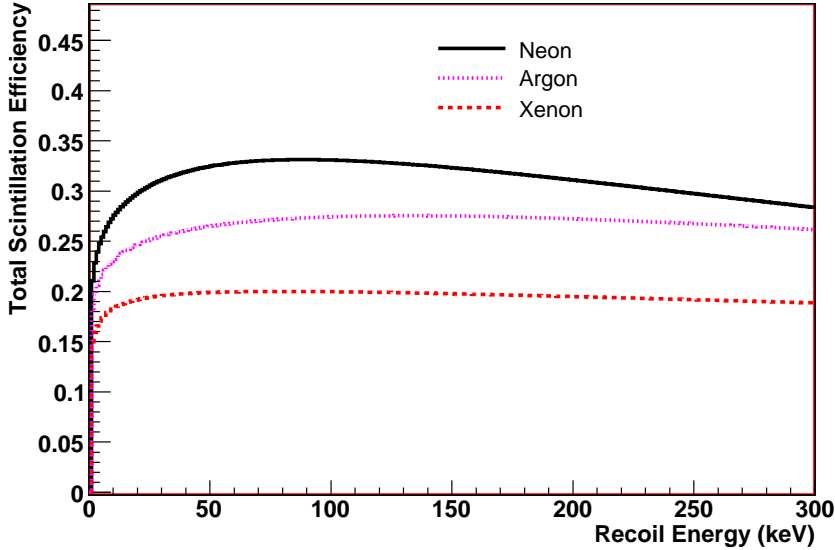


Fig. 6. The total scintillation efficiency for nuclear recoils as a function of recoil energy in liquid neon (black line), argon (red dotted line), and xenon (magenta dashed line).

5 Comparison of model prediction with data

The total scintillation efficiency for each noble liquid, argon, neon, and xenon, is compared to experimental data in Fig. 7, Fig. 8, and Fig. 9. As can be seen, the experimental data can not be explained by Lindhard's theory alone, but can be well described when the Birk's saturation effect has been taken into account. Note that the scintillation efficiencies for 5.035 MeV α particles and 33.5 MeV/amu ^{18}O ions in liquid argon were measured to be 71% and 59% [40,39], which agree very well with our model prediction, 72% and 63%.

It is worthwhile to mention that, although the theoretical uncertainties of electronic stopping power values at very low recoil energy are considerable, the effect on the uncertainties of the final quenching factor are not large as the

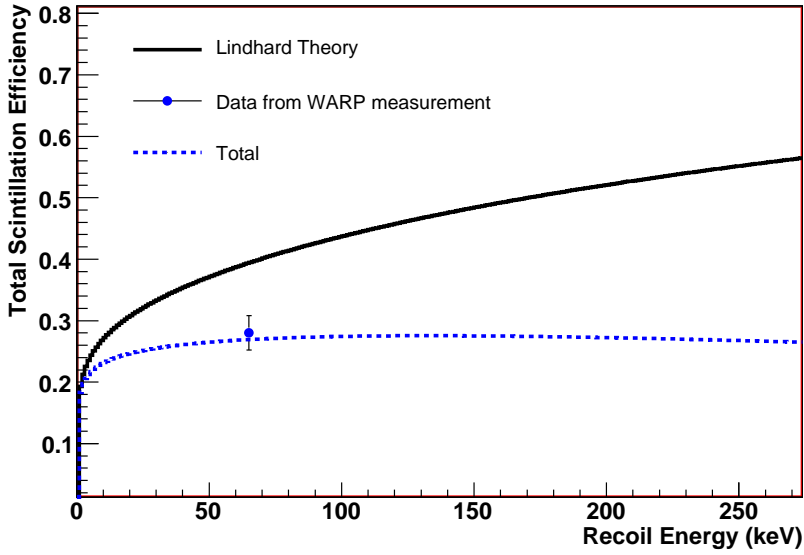


Fig. 7. Argon: a comparison of the total scintillation efficiency (blue curve) calculated by combining two reduction factors to the experimental data [12] in liquid argon. Also shown as the black curve is the Lindhard ionization energy reduction factor.

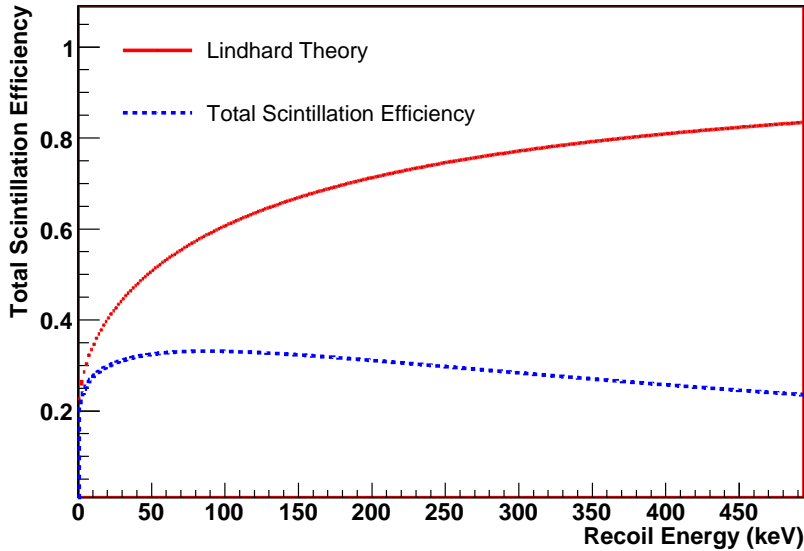


Fig. 8. Neon: the total scintillation efficiency (blue curve) calculated by taking into account two reduction factors is presented in liquid neon.

Birk's constants kB are quite small. For example, by assuming a factor of two difference in the electronic stopping powers at 1 keV in liquid argon, the contribution to the uncertainty of the quenching factor is less than 7%. Thus, the dominant uncertainties come from the uncertainties in the Lindhard theory at very low energy. However, it is usually believed that the Lindhard the-

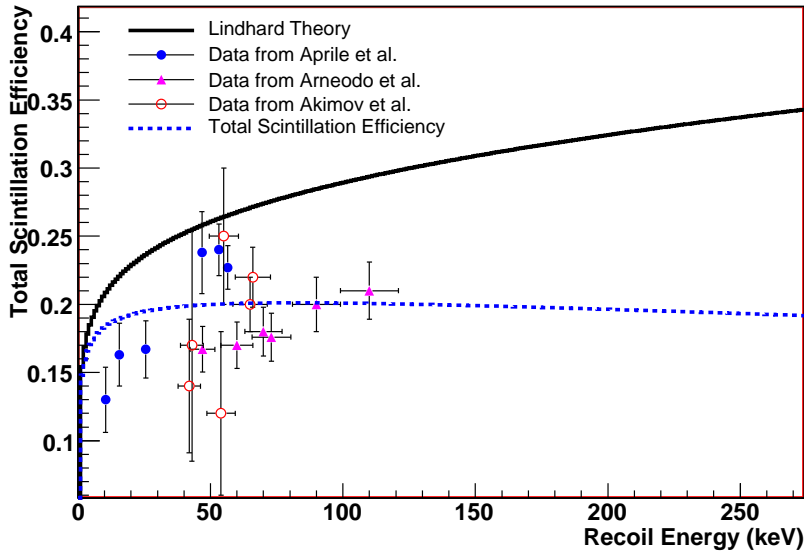


Fig. 9. Xenon: a comparison of the total scintillation efficiency (blue curve) calculated by combining two reduction factors to the experimental data [9,10,11] in liquid xenon. Also shown as the black curve is the Lindhard reduction factor.

ory describes experimental data well [41,42,43,44], although the experimental uncertainties are quite large at low energy.

6 Low-Energy Response to Electrons and γ -rays

Noble liquids' response to low-energy electrons and γ -rays is usually assumed to be linear for the existing experiments [1,3,4]. To investigate whether such an assumption holds, we also calculate and show in Fig. 10 the quenching factor for electronic recoils in liquid argon, neon and xenon utilizing the kB constants determined above. It is clear that the assumption holds quite well down to 20 keV because of the small stopping power values (a few MeV cm²/g) above 20 keV. However, the quenching effect is expected to be significant when the electronic recoil energy is below 20 keV due to the larger stopping power (more than 10 MeV cm²/g).

Note that the kB constants are determined by Birk's law in which the relative scintillation efficiency of nuclear recoils is used, under the assumption that the electronic recoil quenching factor is 1. As we can see in Fig. 10, this assumption is only valid above 20 keV.

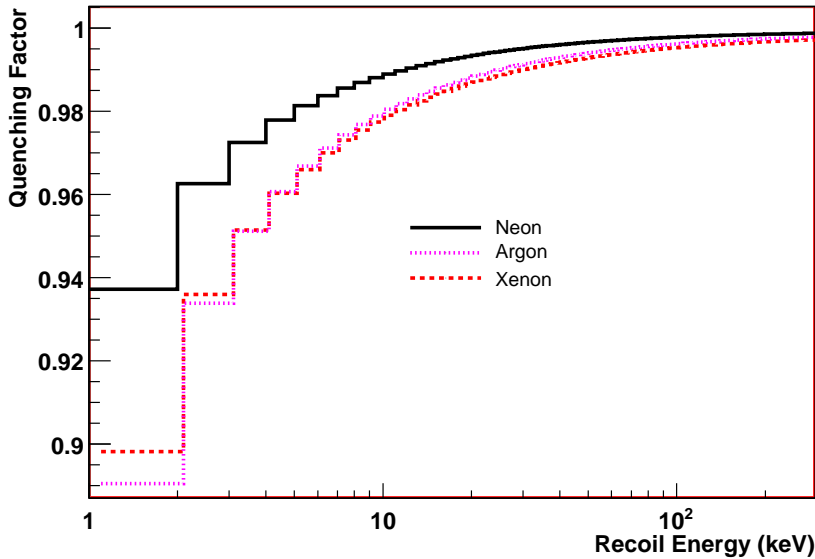


Fig. 10. The quenching factor calculated for electronic recoils in liquid argon (red dotted line), neon (black line), and xenon (magenta dashed line).

7 Conclusion

In summary, we found that the reduced scintillation response to low-energy nuclear recoils comes from two different mechanisms: 1) reduced ionization and excitation energy by nuclear collisions and 2) reduced scintillation photon yield due to high ionization and excitation density induced by nuclear recoils. The former is well described by Lindhard's theory and the latter is attributed to biexcitonic collisions between excitons and the Penning process between excimers. The scintillation quenching induced by the combination of biexcitonic collisions and the Penning process can be described by Birk's law. We have combined these two reduction mechanisms to describe the total scintillation efficiency for noble liquids. The calculations are compared to available data and it is found that they are in good agreement within experimental uncertainties. We have also studied the scintillation response of noble liquid scintillators to low-energy electrons and γ -rays and found that the response is not linear at recoil energy below 20 keV. This paper provides a conventional way to measure the total scintillation efficiency of noble liquids for all types of particles including neutron-induced nuclear recoils, alpha particles and other heavier elements by measuring Birk's constant kB using γ -ray sources.

Acknowledgments

The authors wish to thank the research group at University of South Dakota for the invaluable support that made this work successful. This work was supported in part by the Office of Research at University of South Dakota and by Laboratory Directed Research and Development at Los Alamos National Laboratory. Z.Y. was also partly supported by MOE of China under project No. IRT0624 and the NSFC under grant No. 10635020.

References

- [1] J. Angle *et al.*, astro-ph/0706.0039, submitted to PRL.
- [2] M. G. Boulay and A. Hime, *Astropart. Phys.* **25**, 179 (2006).
- [3] A. Rubbia, *J. Phys. Conf. Ser.* **39**, 129 (2006); Benetti *et al.*, *Nucl. Instr. Meth. A* **574**, 1 (2007).
- [4] D. N. McKinsey *et al.*, *Nucl. Phys. B* **143**, 486 (2005).
- [5] D. N. Spergel *et al.*, *Astrophys. J. Suppl. Ser.* **148**, 175 (2003).
- [6] W. Freeman and M. Turner, *Rev. Mod. Phys.* **75**, 1433 (2003).
- [7] M. W. Goodman and E. Witten, *Phys. Rev. D* **31**, 3059 (1985).
- [8] G. Jungman, M. Kamionkowski, and K. Griest, *Phys. Rep.* **267**, 195 (1996).
- [9] E. Aprile *et al.*, *Phys. Rev. D* **72**, 072006 (2005).
- [10] F. Arneodo *et al.*, *Nucl. Instr. Meth. A* **449**, 147 (2000).
- [11] D. Akimov *et al.*, *Phys. Lett. B* **524**, 245 (2002).
- [12] R. Brunetti *et al.*, *New Astron. Rev.* **49**, 265 (2005).
- [13] R. Brunetti *et al.*, *New Astron. Rev.* **49**, 265 (2005).
- [14] J. A. Nikkel, R. Hasty, W. H. Lippincott, and D. N. McKinsey, astro-ph/0612108 v1; M. G. Boulay, A. Hime and J. Lidgard, nucl-ex/0410025 v1.
- [15] J. Lindhard, *Mat. Fys. Medd. K. Dan. Vidensk. Selsk.* **33**, 1 (1963).
- [16] A. Hitachi, in *Proceedings of the Fourth International Workshop, York, UK, 2002*, edited by Neil J. C. Spooner and Vitaly Kudryavtsev (University of Sheffield, United Kingdom, 2003), P. 357; in *5th International Workshop on the Identification of Dark Matter, IDM2004, Edinburgh, Scotland, 2004* (unpublished).

- [17] Clark, I.D., Masson, A.J. and Wayne, R.P., *Molecular Physics*, **V 23**, 995 (1972).
- [18] C. A. Parker, in *Advances in Photochemistry*, edited by W. A. Noyes, Jr., G. S. Hammond, and J. N. Pitts, Jr. (Interscience, New York, 1964), Vol. 2, p. 305.
- [19] D. C. Lorents, *Physica (Utrecht)* **C 82**, 19 (1976).
- [20] J. B. Birks, *Proc. Phys. Soc.* **A 64**, 511 (1951).
- [21] A. Sayres and C. S. Wu, *Rev. Sci. Instrum.* **28**, 758 (1957).
- [22] A. Hitachi, T. Takahashi, and T. Hamada, *Phys. Rev.* **B 23**, 4779 (1981).
- [23] A. Mozumder, A. Chatterjee, and J. L. Magee, *Advances in Chemical Series 81*, edited by R. F. Gould (American Chemical Society, Washington, DC, 1968), p.27.
- [24] S. Kubota *et al.*, *Phys. Rev.* **B 13**, 1649 (1976); M. Miyajima *et al.*, *Phys. Rev.* **A 9**, 1438 (1974).
- [25] A. Mann and W. Brandt, *Phys. Rev.* **B 24**, 4999 (1981).
- [26] W. Brandt and M. Kitagawa, *Phys. Rev.* **B 25**, 5631 (1982).
- [27] L. Spruch, *Rev. Mod. Phys.* **63**, 151 (1991).
- [28] R. J. Mathar and M. Posselt, *Phys. Rev.* **B 51**, 107 (1995).
- [29] J. F. Ziegler, J. P. Biersack, and U. Littmark, in: *The Stopping and Range of Ions in Matter*, Vol. 1, Pergamon, New York, 1985.
- [30] International Commission on Radiation Units and Measurements, ICRU Report 49, 1993, Bethesda, MD.
- [31] <http://physics.nist.gov/PhysRefData/Star/Text/programs.html>
- [32] J. Lindhard and M. Scharff, *Phys. Rev.* **124**, 128 (1961).
- [33] H. Paul and A. Schinner, *Nucl. Instr. and Meth. in Phys. Res.* **B 179**, 229 (2001).
- [34] Akira Hitachi *et al.*, *Phys. Rev.* **B 27**, 5279 (1983).
- [35] A. Hitachi, T. Doke and A. Mozumder, *Phys. Rev.* **B 46**, 11463 (1992).
- [36] S. Kubota *et al.*, *Phys. Rev.* **B 13**, 1649 (1976).
- [37] Robert S. Mulliken, *J. Chem. Phys.* **52**, 5170 (1970).
- [38] M. Martin, *J. Chem. Phys.* **54**, 3289 (1971).
- [39] Jay A. LaVerne *et al.*, *Phys. Rev.* **B 54**, 15724 (1996).
- [40] T. Doke *et al.*, *Nucl. Instr. and Meth. in Phys. Res.* **A 269**, 291 (1988).
- [41] A. R. Sattler, F. L. Vook and J. M. Palms, *Phys. Rev.* **143**, 588 (1966).

- [42] C. Chasman *et al.*, Phys. Rev., **154**, 239 (1967).
- [43] T.Schutt *et al.*, Phys. Rev. Lett. **69**, 24 (1992).
- [44] G. Gerbier *et al.*, Phys. Rev. D **42**, 9 (1990).